EFDA–JET–CP(14)06/02

J. Garcia, J. Citrin, T. Goerler, N. Hayashi, F. Jenko, P. Maget,
P. Mantica, M.J. Pueschel, D. Told, C. Bourdelle, R. Dumont, G. Giruzzi,
G.M.D. Hogeweij, S. Ide, T. Johnson, H. Urano, the JT-60U Team
and JET EFDA contributors

# Core Microturbulence and Edge MHD Interplay and Stabilization by Fast Ions in Tokamak Confined Plasmas

"This document is intended for publication in the open literature. It is made available on the understanding that it may not be further circulated and extracts or references may not be published prior to publication of the original when applicable, or without the consent of the Publications Officer, EFDA, Culham Science Centre, Abingdon, Oxon, OX14 3DB, UK."

"Enquiries about Copyright and reproduction should be addressed to the Publications Officer, EFDA, Culham Science Centre, Abingdon, Oxon, OX14 3DB, UK."

The contents of this preprint and all other JET EFDA Preprints and Conference Papers are available to view online free at www.iop.org/Jet. This site has full search facilities and e-mail alert options. The diagrams contained within the PDFs on this site are hyperlinked from the year 1996 onwards.

# Core Microturbulence and Edge MHD Interplay and Stabilization by Fast Ions in Tokamak Confined Plasmas

J. Garcia[1], J. Citrin[1,2], T. Goerler[3], N. Hayashi[4], F. Jenko[3], P. Maget[1], P. Mantica[5], M.J. Pueschel[6], D. Told[3], C. Bourdelle[1], R. Dumont[1], G. Giruzzi[1], G.M.D. Hogeweij[2], S. Ide[4], T. Johnson[7], H. Urano[2], the JT-60U Team and JET EFDA contributors*

***JET-EFDA, Culham Science Centre, OX14 3DB, Abingdon, UK***

*[1]CEA, IRFM, F-13108 Saint-Paul-lez-Durance, France.*
*[2]FOM Institute DIFFER – Dutch Institute for Fundamental Energy Research – Association EURATOM-FOM, Nieuwegein, The Netherlands*
*[3]Max Planck Institute for Plasma Physics, EURATOM Association, Boltzmannstr. 2, 85748 Garching, Germany*
*[4]Japan Atomic Energy Agency, Mukouyama, Naka City, Ibaraki, 311-0193 Japan*
*[5]Istituto di Fisica del Plasma "P. Caldirola", Associazione Euratom-ENEA-CNR, Milano, Italy*
*[6]University of Wisconsin-Madison, Madison, Wisconsin 53706, USA*
*[7]Euratom-VR Association, EES, KTH, Stockholm, Sweden*
** See annex of F. Romanelli et al, "Overview of JET Results", (25th IAEA Fusion Energy Conference, St Petersburg, Russia (2014)).*

Preprint of Paper to be submitted for publication in Proceedings of the 25th IAEA Fusion Energy Conference, St Petersburg, Russia
13th October 2014 - 18th October 2014

**ABSTRACT**

Extensive linear and non-linear gyrokinetic simulations and linear MHD analyses performed for two JET hybrid discharges have shown that the large population of fast ions found in the plasma core under particular heating conditions has a strong impact on core microturbulence and edge MHD by reducing core ion heat fluxes and increasing pedestal pressure in a feedback mechanism. This mechanism is found to be highly dependent on plasma triangularity as it changes the balance between the improvement in the plasma core and the edge. The feedback mechanism plays a similar role in the ITER hybrid scenario as in the JET discharges analyzed due to its high triangularity plasmas and the large amount of fast ions generated in the core by the heating systems and the alpha power.

## 1. INTRODUCTION

The tokamak concept aims for the confinement of high temperature plasmas by magnetic fields. However, the high thermal energy confined is degraded by two main mechanisms: small-scale instabilities (microturbulence), and by larger-scale instabilities that can be described by MagnetoHydroDynamics (MHD). Microturbulence driven by ion temperature gradients, referred to as the Ion Temperature Gradient (ITG) mode [1], are driven linearly unstable when the logarthimic ion temperature gradients are above a critical threshold, defined by $R/L_{Ti} > R/L_{Ti,crit}$, where $L_{Ti} = T_i / \nabla T_i$ is the ion temperature gradient length and the tokamak major radius R is a normalizing factor. ITGs are typically responsible for the ion heat transport observed in confined plasmas under standard conditions, while MHD significantly restricts the access to high plasma pressure when the magnetic topology is broken at some critical pressure or pressure gradient values. Therefore, reducing the impact of these transport mechanisms is a key point in order to increase the energy confinement time in magnetically confined plasmas.

Hybrid or advanced inductive scenarios [2], characterized by high confinement, have high pressure with limited or few MHD events and therefore may extrapolate promisingly to future fusion reactor devices. The improved confinement is likely due to stability improvements both in the plasma core and at the edge, where a higher pedestal confinement is obtained compared to the standard inductive H-mode scenarios. The importance of fast ions for obtaining hybrid regimes, has been already pointed out for JET plasmas [3] where it was shown that these particles substantially contributed to the high pressure and pressure gradients typical of those regimes, and made the plasma less paramagnetic (or more diamagnetic) by significantly increasing $\beta_p = 2\mu_0 < P > < B_\theta^2 >$, with <P> the average pressure and $B_\theta$ the poloidal magnetic field, to the $\beta_p \geq 1$ region, which is expected for hybrid regimes at JET [4,5]. It was also shown that there is interplay between the core and edge regions which drives the improved confinement. However, the exact physical mechanisms which allow the appearance of high pressure gradients and the interplay with fast ions and the edge were still mostly unknown. Previous linear microinstability analysis has already shown that fast ions can stabilize ITG modes in the plasma core due to the fast ion dilution in

thermal species [6], the modification of Shafranov-shift [7] or the electromagnetic stabilization due to a local increase of the pressure gradient [8], which is enhanced non-linearly [9]. However, none of these effects can explain by themselves the increased confinement in the edge region obtained in advanced inductive scenarios, like JET [10], and how that improvement affects the core. Actually, the high thermal pressure obtained in advanced inductive scenarios is mainly achieved because of the high pressure at the edge, as both are highly correlated. However, whether an improvement in the edge stability leads to a higher core pressure or an increase in pressure is a cause for improved edge stability is something that has not been yet clarified.

In this paper, two hybrid JET shots, with significant thermal improved confinement and fast ion content, are analyzed to assess the previous points. For that purpose, detailed linear and non-linear gyrokinetic and linear MHD simulations are performed at the core and edge plasma regions. The results show how – unlike thermal particles – a large population of fast ions is a key ingredient for a positive feedback between plasma core and edge which can improve thermal energy confinement in both regions.

The paper is organized as follows: in section 2 the experimental discharges studied are discussed. In section 3 the impact of fast ions in microturbulence is analyzed, and in section 4 their impact on edge MHD and the onset of a feedback with the core is discussed. In section five, an extrapolation to ITER is shown. Finally some conclusions are discussed in section 6.

## 2. EXPERIMENTAL DATA

Two representative discharges of JET hybrid scenarios, discharge Pulse Number: 75225 [9] at low triangularity, and Pulse Number: 77923, at high triangularity, were analyzed. The time evolution of the main parameters is shown in figure 1 whereas a full summary is found in Table I. In both cases, a high input Neutral Beam Injection (NBI) power is combined with low average density and Greenwald fraction for achieving both a high beta, $\beta = 2\mu_0 < P > / B^2$, where B is the magnetic field, as well as a thermal energy enhancement factor relative to the IPB98(y,2) scaling, $H_{98}(y,2)$, higher than 1. The remarkable difference between the two discharges is the upper triangularity: $\delta_u = 0.16$ for Pulse Number: 75225 and $\delta_u = 0.38$ for Pulse Number: 77923. This is visible from the EFIT calculated magnetic equilibrium, as shown in figure 1, and has an impact on the overall plasma behavior. Whereas the $H_{98}(y,2)$ factor is similar in both cases, the average density and the pedestal pressure are both higher for Pulse Number: 77923. This feature has an impact on the core profiles as well as on the fast ions generated by the NBI system. In particular, the ion temperature has a steepened profile at $\rho = 0.33$ for Pulse Number: 75225, $R/L_{Ti} = 6.25$, however $R/L_{Ti} = 5.7$ for Pulse Number: 77923. In order to assess the possible differences on the fast ion distribution for both discharges, interpretative simulations were carried out with the CRONOS [11] suite of integrated modeling codes. The fast ion content for NBI-driven fast ions was calculated by orbit following Monte Carlo codes, NEMO/SPOT [12]. The q profile used for the calculations was obtained by equilibrium reconstructions constrained by MSE angles and total pressure. In figure 2,

the total, thermal, and fast ion pressures, as well as the fast ion and electron density profiles, and the magnetic equilibrium are shown for both discharges. The fast particles change the total plasma energy content by changing the core pressure profile. This change is stronger for Pulse Number: 75225, as the normalized beta rises from $\beta_{N,th}^{75225} = 2.13$ to $\beta_N^{75225} = 2.9$ whereas for Pulse Number: 77923 it is from $\beta_{N,th}^{77923} = 2.46$ to $\beta_N^{77923} = 2.8$. The ratio of thermal and fast ion densities is also modified as $n_{fast}/n_e \sim 0.13$ for Pulse Number: 75225 and $n_{fast}/n_e \sim 0.05$ for Pulse Number: 77923 at $\rho = 0.33$, being $\rho$ the normalized toroidal magnetic flux. The difference on the fast ion population has an impact on magnetic equilibrium and in particular on the Shafranov-shift, as shown in figure 2, which increases by $\Delta_{75225}^{Shafranov-Shift} \approx 4.0cm$ whereas the increase is more modest for Pulse Number: 77923, $\Delta_{77923}^{Shafranov-Shift} \approx 2.0\,cm$. Finally, the pressure gradient in the core region is also modified. A parameter of merit of the local pressure modification is $\alpha = -Rq^2 d\beta/dr$, which increases from $\alpha_{th}^{75225}(\rho = 0.33) = 0.35$ up to $\alpha^{75225}(\rho = 0.33) = 0.52$ and $\alpha_{th}^{75225}(\rho = 0.33) = 0.28$ up to $\alpha^{75225}(= 0.33) = 0.34$ .The impact of the fast ions for both discharges, and the analysis of the similitudes and differences will be analyzed in the following sections.

## 3. MICTROTURBULENCE ANALYSIS

The impact of the fast ions on core microturbuelnce is analyzed by means of the GENE gyrokinetic code [13]. Gene solves the gyrokinetic Vlasov equation, coupled self-consistently to Maxwell's equations, within a *δf* formulation. Gene works in field line coordinates, where x is the radial coordinate, z is the coordinate along the field line, and y is the binormal coordinate. All simulations carried out were local. The geometry used was calculated by HELENA based on the interpretative analysis of the discharges. Collisions are modeled using a linearized Landau-Boltzmann operator. Both linear and nonlinear initial value simulations were performed. Typical grid parameters were as follows: perpendicular box sizes [Lx,Ly] = [250,125] in units of ion Larmor radii, perpendicular grid discretization [nx, nky] = [256,32], 32 point discretization in the parallel direction, 48 points in the parallel velocity direction, and 12 magnetic moments. The high Lx and nx values were necessary to satisfy the boundary conditions in the low magnetic shear simulations at low radii. Parallel magnetic fluctuations were included in the simulations. This cannot be neglected, due to the relatively high $\beta$, and is important for setting the strength of electromagnetic coupling, as seen in dedicated checks.

The turbulent linear growth rates $\gamma$ and flow shear rate, $\gamma_E$, are in units of $c_s/R$, with $c_s = \sqrt{T_e/m_i}$ and $m_i$ the main ion mass. The fast particle distribution function was approximated as Maxwellian, taking the average energy of the fast ion slowing-down distribution as the temperature found to be $T_{fast}$ = 35keV for Pulse Number: 75225 and $T_{fast}$ = 27keV for Pulse Number: 77923. For the gyrokinetic calculations excluding the energetic ions, the equilibrium was recalculated with only the thermal pressure, and then used for the simulations. The dimensionless parameters of the discharge at $\rho = 0.33$ fed into the gyrokinetic calculations are summarized in Table II. The selected time for Pulse Number: 75225 is t = 6.03s and t = 7s for Pulse Number: 77923.

In Figure 3, the linear growth rates and frequencies are shown for the nominal experimental value of $R/L_{Ti} = 6.25$ for various assumptions in the input parameters for the discharge Pulse Number: 75225. In order to identify the nature of the underlying modes, the ExB flow shear rate was set to zero. Over a wide normalized wavenumber range, $k_y = k_y\rho_s$ where $\rho_s$ is the ion gyroradius with respect to the sound speed, ITG modes are unstable. The maximum growth rate is reduced by ≈ 30% when including fast ions in the system. When including the nominal fast ion pressure gradient, an additional mode is apparent at $k_y = 0.1–0.15$. This mode is stabilized when reducing the fast ion pressure gradient by 30% and it has a significantly higher frequency than the ITG modes, at $\omega \approx 2.5$. This is within 5% of the corresponding GAM frequency as determined by a Rosenbluth-Hinton test. This mode is identified as a β-induced Alfvén Eigenmode (BAE) [14], which is known to be degenerate with the GAM frequency and destabilized by fast ions. This mode share characteristics and has similar frequency as the Kinetic Ballooning Modes (KBM), and we will refer to it as a generalized BAE/KBM electromagnetic mode. Therefore, at this radial position, the turbulence regime is found to be in the direct vicinity of the ITG-BAE/KBM boundary. A nonlinear $R/L_{Ti}$ scan with and without fast ions, is shown in Figure 3. The reduced fast ion pressure gradient is maintained throughout this scan. This is consistent with an assumption that the fast ion pressure is clamped by the manifestation of the BAE-like modes which are known to drive fast ion transport. This reduced fast ion pressure gradient can be obtained from the SPOT modeling when assuming a fast ion diffusion coefficient of $D_{fast} = 0.5m^2/s$. This agrees with the nonlinear GENE predicted fast ion transport at the nominal $R/L_{Ti}$ as seen in Figure 3, *a posteriori* justifying the assumption.

The experimental toroidal rotation was taken into account by including the ExB flow shear rate, $\gamma_E = 0.2$, and the according parallel flow shear. The heat flux obtained is normalized by the gyroBohm normalization factor, $q_{GB} = T_i^{2.5} n_i m_i^{0.5}/e^2 B^2 R^2$, with $n_i$ is the ion density. Here, the fast ions provide an improvement of ≈ 10–25% on $R/L_{Ti}$ for the same heat flux. When including fast ions, the ion heat flux rapidly increases for $R/L_{Ti} > 7.2$ and the fast ions are no longer stabilizing. This is correlated with a significant increase in the fast ion transport. Linear analysis shows that the BAE/KBM modes are destabilized in this high $R/L_{Ti} > 7.2$ regime, even with the reduced fast pressure gradient. These modes have a strong resonant interaction with both thermal and energetic ions. The consistency of the simulation output and power balance values, in a BAE/KBM marginal regime, suggests that a self- limitation mechanism may be active, whereby the fast ion pressure gradient is maintained at a level consistent with BAE marginality.

The impact of the fast ions has been as well analyzed for the discharge 77923. In Figure 4, the linear growth rates and frequencies are shown for the nominal experimental value of $R/L_{Ti} = 5.7$. Unlike the previous case, no BAE/KBM modes are obtained and only ITG modes are unstable in a narrow $k_y = 0.2–0.45$ region. This is consistent with the fact the pressure gradient is lower and the magnetic shear higher for this discharge at the selected point. In order to demonstrate that the BAE/KBM limit is indeed different for both discharges a scan on $\beta_e$ has been performed

and shown in figure 4. In spite of the fact that both discharges have similar β, the discharge Pulse Number: 75225 lies at the boundary between ITG and BAE/KBM whereas the Pulse Number: 77923 is at 60%.

The maximum growth rate is reduced by 30% when the fast ions are included in this case, a value similar to the one obtained for the low triangularity discharge. A nonlinear $R/L_{Ti}$ scan was performed as well with and without fast ions, as shown in Figure 4. The experimental toroidal rotation was taken into account by including the *ExB flow* shear rate, $\gamma_E = 0.15$, and the according parallel flow shear. Here, the fast ions provide an improvement of 10% of the heat flux, in the range of $R/L_{Ti}$ analyzed. The agreement between the heat flux obtained and the one calculated from power balance is still quite good. For this discharge, the improved heat flux at the experimental $R/L_{Ti}$ is lower than for the discharge Pulse Number: 75225, which reached 25%. One possible reason is the closeness to the KBM limit. As shown in figure 4 and in [15], the ITG stabilization by electromagnetic effects is stronger when the plasma is closer to the KBM/BAE limit.

In order to analyze the influence of the electromagnetic effects and the role of the flow shear in these discharges, different non-linear simulations were performed by reducing the nominal $\beta_e$ by a factor $10^{-3}$ in both cases. Additionally, two extra simulations for both discharges, one with no ExB and another one with three times the nominal ExB, were performed. Results, shown in figure 5 show the electromagnetic effects are essential to obtain the correct ion heat fluxes for both discharges as they significantly increase by if they are neglected. Regarding the ExB flow shear, its effect tend to be negligible or even destabilizing when the full electromagnetic simulation is performed, however it is stabilizing for the electrostatic simulation. This confirms that the electromagnetic effects together with the fast ions have a significant stabilization effect in the plasma core, much more than ExB shear flow.

## 4. EDGE MHD ANALYSIS AND CORE-EDGE INTERPLAY

We now analyze the edge stability. The peeling-ballooning diagram was calculated following the procedure detailed in Ref [16]. The MHD code MISHKA [17] was used for computing lineal ideal MHD stability at the edge. For this purpose, as previously, the equilibrium was calculated with and without fast ions. In the peeling-ballooning diagram, shown in figure 5 for both discharges, the experimental pedestal pressure is well predicted by the calculations and the experimental value lies on the ballooning side. This good agreement is obtained when the fast ion pressure is included, as it extends the stable region for both discharges. However, there is a fundamental difference between both discharges. Whereas the core fast ion pressure for the discharge Pulse Number: 75225, which is 30% of the total energy, increases the stable region by 10%, for the discharge Pulse Number: 77923, with just a 10% of fast ion energy, the stable region increases by 15%. This shows the importance of the high triangularity configuration for taking advantage of the stabilization of the pedestal by increasing β. It is worth to point out that, due to the plasma stiffness, even a modest improvement of the pedestal can lead to a higher overall improved

thermal confinement than microturbulence improvement in the core, as the volume affected is much higher.

A rough analysis of the interplay between core and edge has been studied by performing non-linear simulations for both discharges at 5% lower $\beta_e$, assuming that a 10% reduction of pedestal pressure obtained by removing the fast ion content leads to a 5% less electron pressure in the core through stiffness. As shown in figure 3 and 4, the ion heat flux increase for both discharges up to 10% due to lower electromagnetic stabilization of ITG modes.

In order to show how the fast ions are a key ingredient for both a microturbulence improvement in the core and a pedestal pressure at the edge, an alternative gyrokinetic calculation was carried out. The fast ion content was removed for the discharge Pulse Number: 75225 and the thermal electron and ion content and gradients were increased such that $\beta_N$ and $\alpha$ are maintained, whereas the plasma geometry is also kept constant. In these two cases the pedestal would behave exactly the same as the Shafranov-shift is the same. The new growth rates, shown in figure 5, increase throughout the spectrum, and its maximum is 2.5 times higher compared to the case with fast ions, which would result in a much higher heat flux. The key point is that the fast ions, unlike thermal particles, increase pressure in the plasma core, while simultaneously not contributing to the ITG drive and even stabilizes it (which can lead to higher thermal pressure as the ion temperature also increases). Therefore under the same conditions, in particular the same input power, a particular level of Shafranov-shift (or of pedestal improvement) is achieved much more efficiently in the presence of a high fast ion population than with pure thermal particles. Increased thermal content also increases core microturbulence limiting the global $\beta$ obtained and therefore also limiting the possible pedestal pressure attained. Finally, for these shots the relative weight of the effects varies. In the core the fast ions and electromagnetic effects have a stronger impact for Pulse Number: 75255 due to the lower density and vicinity to the KBM/BAE boundary. However the impact of the suprathermal pressure for edge enhancement is lower due to the low triangularity On the other hand, for Pulse Number: 77923, the trend is the opposite. The global effect could be eventually the same for both discharges, however, self-consistent simulations are required in order to confirm this point.

## 5. ITER ANALYSIS

With the aim of analyzing if the same effect can play a role in tokamaks with low external torque, as ITER, the same procedure has been applied to a typical ITER hybrid scenario [18] with the characteristics shown in table 1. The suprathermal pressure from all the power sources is shown in figure 7. Although the fast ion densities associated with the fusion $\alpha$-particles and with the NBI beams are low, $n_{fast,\alpha}/n_e \sim 0.009$ and $n_{fast,beams}/n_e \sim 0.006$, their pressure (and pressure gradient), is not negligible as their energy is quite high, $T_{fast,alpha} = 1.1$MeV and $T_{fast,beams} = 0.55$MeV which increases $\beta_{N,th} = 2.5$ up to $\beta_N = 3.0$. Microturbulence, calculated at $\rho = 0.33$, is found to be ITG and also modified by these fast ions with a growth rate reduction of up to 30%. The increased $\beta$

also expands the stable peeling-ballooning region at the edge, similarly as obtained for JET (up to 10%). This represents a significant increase of fusion power, which in turn would also increase β in a positive feedback.

The fact that the mechanism discussed in this paper has the same impact in ITER than in JET comes from the fact that ITER gets a maximum benefit from the core fast ions, due to the high population of α-particles and from the stabilization of the pedestal, because of the high triangularity. Therefore, the ITER hybrid behaves as a mixture of JET low and high triangularity plasmas. This implies that, unlike rotational flow shear, the role played by fast ions in ITER and future tokamak reactors can have the same impact as in present day experiments, primarily due to the α-particles, which will be the main heating mechanism.

## 6. CONCLUSIONS

We have presented evidence of the simultaneous modification by fast ions of microturbulence and MHD by performing gyrokinetic and MHD analyses to two JET hybrid shots at high and low triangularity. In the core, mictroturbulence is reduced by fast ions when electromagnetic effects are taken into account whereas the ExB flow shear has been shown to play a minor effect. At the same time, the fast ions increase the total core pressure without increasing the turbulence drive. This leads to an improved edge pedestal pressure by means of the increased Shafranov-shift in a manner unachievable by pure thermal pressure, which is strongly limited by microturbulence. A positive core-edge feedback is therefore established and it is expected to be efficient until BAE/KBM modes are destabilized due to the strong plasma pressure gradient obtained, which would increase both thermal and fast ion transport. However, it has been shown that this interplay is highly dependent on the magnetic geometry as the relative improvement in the core and at the edge, and their interplay, depends on triangularity and plasma density. In ITER and fusion reactors, this effect can play a similar role as in present day experiments, owing to the high level of fast ions born from fusion reactions, which highly increase the pressure gradient in the plasma core, and therefore can compensate for the low rotation expected due to the high density required for producing sufficient fusion energy.

## ACKNOWLEDGEMENTS

This work was supported by EURATOM and carried out within the framework of the European Fusion Development Agreement. The views and opinions expressed herein do not necessarily reflect those of the European Commission. This work has been carried out within the framework of the EUROfusion Consortium and has received funding from the European Union's Horizon 2020 research and innovation programme under grant agreement number 633053. The views and opinions expressed herein do not necessarily reflect those of the European Commission. Numerical simulations were performed at IFERC-CSC

## REFERENCES


[1]. F. Romanelli, Physics of Fluids B **1**, 1018 (1989).

[2]. T.C. Luce et al., Nuclear Fusion **43**, 321 (2003).

[3]. J. Garcia and G. Giruzzi Nuclear Fusion **53**, 043023 (2013).

[4]. M.N.A. Beurskens et al 2013 Nuclear Fusion **53** 013001

[5]. J. Garcia and G. Giruzzi, Physical Review Letters **104**, 205003 (2010).

[6]. G. Tardini et al. Nuclear Fusion **47**, 280 (2007).

[7]. C. Bourdelle, et al., Nuclear Fusion **45**, 110 (2005).

[8]. M. Romanelli et al., Plasma Physics and Controlled Fusion **52**, 045007 (2010).

[9]. J. Citrin et al., Physical Review Letters **111**, 155001 (2013).

[10]. J. Hobirk et al., Plasma Physics and Controlled Fusion **54** 095001 (2012).

[11]. J.F. Artaud et al., Nuclear Fusion **50**, 043001 (2010).

[12]. M. Schneider et al., Nuclear Fusion **51**, 063019 (2011).

[13]. F. Jenko, W. Dorland, M. Kotschenreuther and B.N. Rogers, Physics of Plasmas **7**, 1904 (2000).

[14]. F. Zonca et al., Plasma Physics and Controlled Fusion **38**, 2011 (1996).

[15]. J. Citrin et al. submitted to Plasma Physics and Controlled Fusion.

[16]. P. Maget et al., Nuclear Fusion **53** 093011 (2013).

[17]. G.T.A. Huysmans et al., Plasma Physics and Controlled Fusion **8** 4292 (2001).

[18]. K. Bassiguir et al., Plasma Physics and Controlled Fusion **55**, 125012 (2013).


| Shot | Ip (MA) | Bt (T) | $q_{95}$ | $\kappa/\delta$ | $\beta_N/\beta_{N,th}$ | $H_{98}(y,2)$ | $P_{tot}$(MW) | $\omega_{tor}$(krad/s) |
|---|---|---|---|---|---|---|---|---|
| 75225 | 1.7 | 2.0 | 4.0 | 1.64/0.23 | 2.93/2.13 | 1.30 | 17 | 76.7 |
| 77923 | 1.7 | 2.0 | 4.0 | 1.70/0.38 | 2.80/2.46 | 1.30 | 21 | 63.2 |
| ITER | 12 | 5.3 | 4.30 | 1.80/0.40 | 3.0/2.50 | 1.30 | 73 | ~0 |

*TABLE I: Main characteristics of the discharges analyzed in this letter. Ip is the total current, Bt the toroidal magnetic field, κ elongation, δ triangularity, $\beta_N = \beta aB/Ip$ normalized beta ((with a the plasma minor radius), $\beta_{N,th}$ normalized thermal beta, $H_{98}(y,2)$ thermal confinement factor, $P_{tot}$ injected power and $\omega_{tor}$ angular rotation.*

| Shot | s | q | Te/Ti | $R/L_{Ti}$ | $R/L_{Te}$ | $R/L_{Ne}$ |
|---|---|---|---|---|---|---|
| 75225 | 0.15 | 1.16 | 0.67 | 6.2 | 4.3 | 2.6 |
| 77923 | 0.22 | 1.09 | 0.87 | 5.7 | 4.6 | 1.14 |
| ITER | 0.24 | 1.17 | 1.09 | 3.4 | 2.9 | 1.9 |

*TABLE II: Discharge dimensionless parameters at $\rho = 0.33$ used as input in simulations*

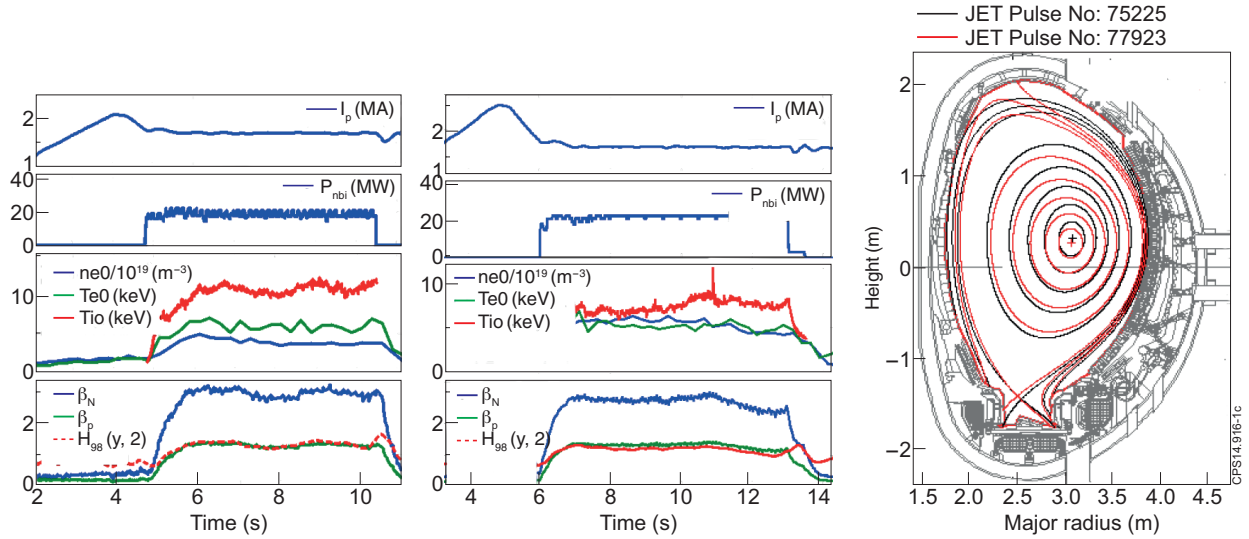


*Figure 1: Time evolution for discharge Pulse Number: 75225 (left), for Pulse Number: 77923 (center), and the EFIT calculated magnetic equilibrium for both shots (right).*

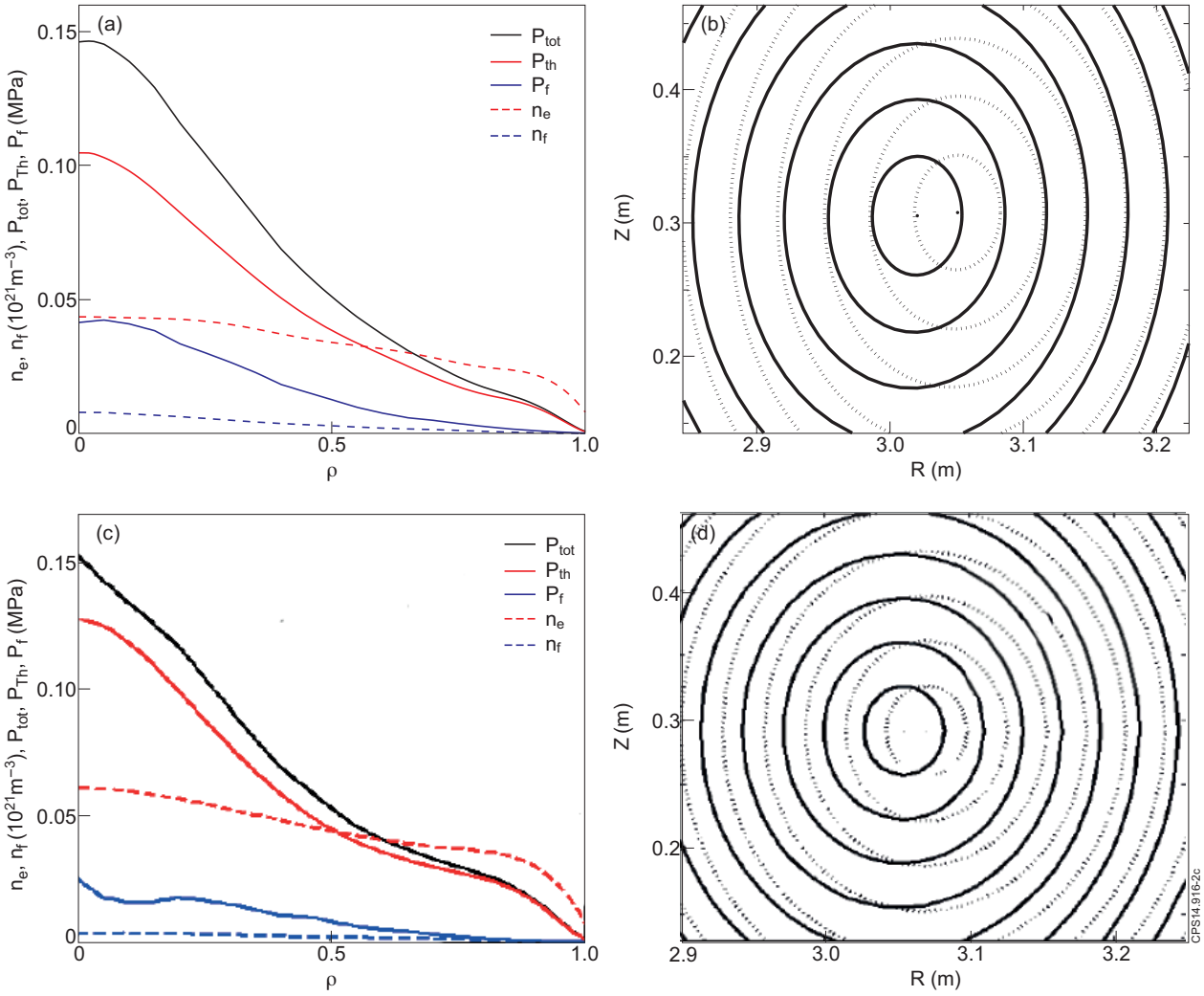


*Figure 2: Total (Ptot), thermal (Pth), fast ion (Pf) pressure and electron (ne) and f st ion (nf) density profiles for the shots 75225 (a) and 77923 (c). Plasma equilibrium with fast ions (dashed) and without fast ions (solid) for the shots 75225 (b) and 77923 (d).*

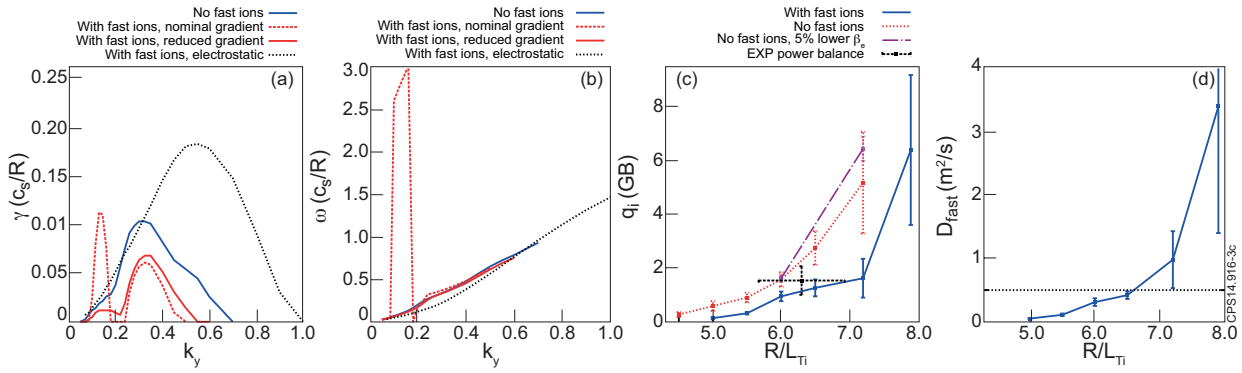


*Figure 3: Linear growth rates and frequencies for discharge 75225 (a,b) Ion heat flux and fast ion particle diffusivity from nonlinear gyrokinetic simulations (c,d). The analysis was carried out at $\rho = 0.33$.*

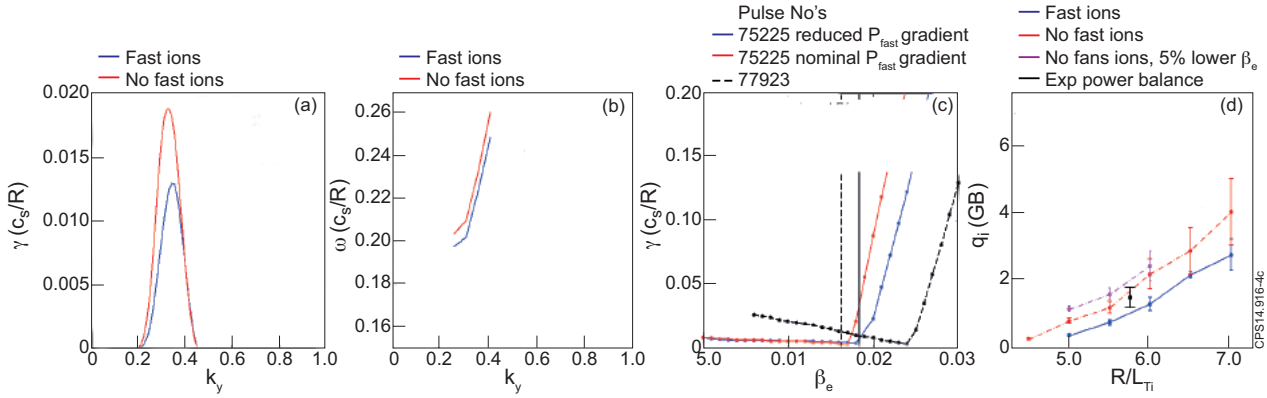


*Figure 4: Linear growth rates and frequencies for discharge 77923 (a,b) Linear growth rate dependence on $\beta_e$. Vertical lines represent experimental data for 77923 (dashed) and 75225 (solid) (c). Ion heat flux from nonlinear gyrokinetic simulations (d). The analysis was carried out at $\rho = 0.33$.*

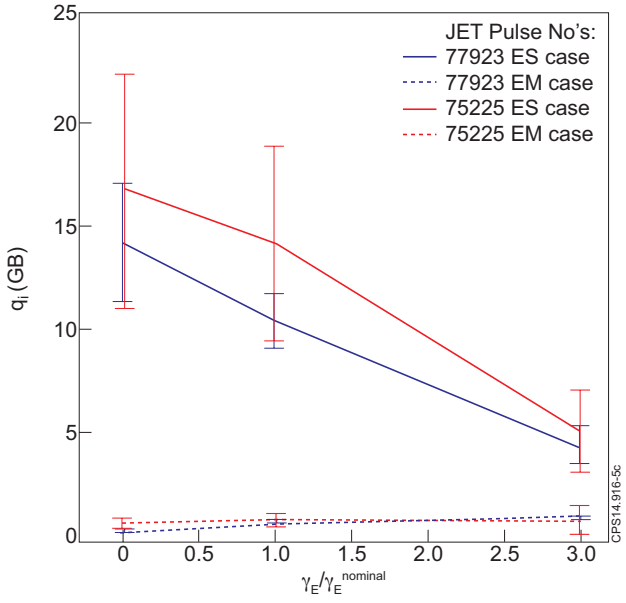


*Figure 5: Ion heat flux dependence on $\gamma_E$ in the case of electrostatic case (ES) and electromagnetic case (EM).*

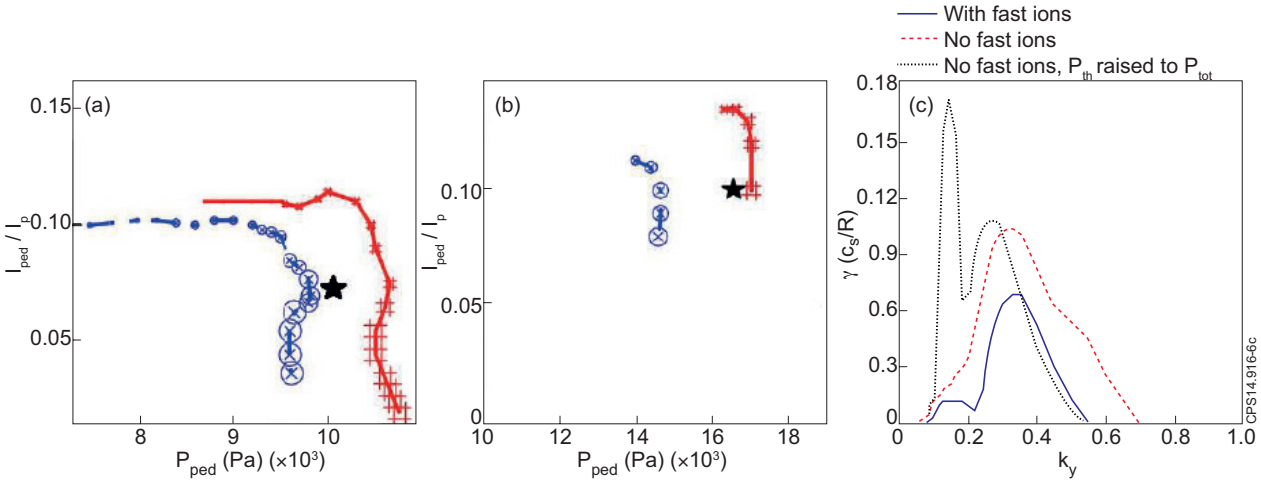


*Figure 6: Peeling-ballooning boundaries for discharges 75225 (a) and 77923 (b). The experimental value is marked with a star. Large or small symbols indicate high or low toroidal mode number respectively. Linear growth rates with and without fast ions and with artificially increased thermal pressure (c).*

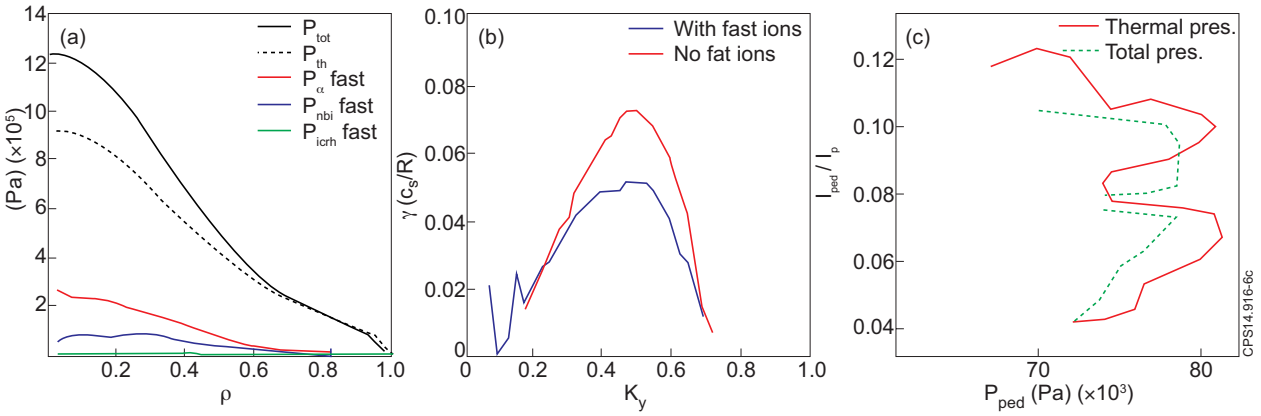


*Figure 7: Total (Ptot), Thermal (Pth), alpha fast ion (Palpha fast), nbi fast ion (Pnbi fast) and Ion Cyclotron Resonant Heating (ICRH) fast ion (Picrh fast) pressure profiles (left). Linear growth rates with and without fast ions for the ITER hybrid scenario at ρ = 0.33 (center). Peeling-ballooning boundaries with and without fast ions for ITER (right).*